The Journal of Immunology
RESEARCH ARTICLE | JULY 17 2024

Monoclonal Antibodies Engineered with Fc Region Mutations to Extend Protection against Fentanyl Toxicity FREE

Aaron Khaimraj; ... et. al

J Immunol (2024) 213 (5): 663–668.
https://doi.org/10.4049/jimmunol.2400170

Monoclonal Antibodies Engineered with Fc Region Mutations to Extend Protection against Fentanyl Toxicity

Aaron Khaimraj,* Carly A. Baehr,* Dustin Hicks,* Michael D. Raleigh,* and Marco Pravetoni[†,‡]

Fentanyl and other synthetic opioids are the leading cause of drug-related deaths in the United States. mAbs that selectively target fentanyl and fentanyl analogues offer a promising strategy for treating both opioid-related overdoses and opioid use disorders. To increase the duration of efficacy of a candidate mAb against fentanyl, we selected three sets of mutations in the Fc region of an IgG_1 anti-fentanyl mAb (HY6-F9^{DF215}, HY6-F9^{DHS}, HY6-F9^{YTE}) to increase binding to the neonatal Fc receptor (FcRn). The mAb mutants were compared against unmodified (wild-type [WT], HY6-F9^{WT}) anti-fentanyl mAb for fentanyl binding, thermal stability, and FcRn affinity in vitro, and for efficacy against fentanyl and mAb half-life in vivo in mice. Biolayer interferometry showed a >10-fold increase in the affinity for recombinant FcRn of the three mutant mAbs compared with HY6-F9^{WT}. During an acute fentanyl challenge in mice, all FcRn-mutated mAbs provided equal protection against fentanyl-induced effects, and all mAbs reduced brain fentanyl levels compared with the saline group. Serum persistence of the mutant mAbs was tested in Tg276 transgenic mice expressing human FcRn. After administration of 40 mg/kg HY6-F9^{WT}, HY6-F9^{DF215}, HY6-F9^{DHS}, and HY6-F9^{YTE}, the mAbs showed half-lives of 6.3, 26.4, 14.7, and 6.9 d, respectively. These data suggest that modification of mAbs against fentanyl to bind to FcRn with higher affinity can increase their half-life relative to WT mAbs while maintaining efficacy against the toxic effects of fentanyl, further supporting their potential role as a therapeutic treatment option for opioid use disorder and overdose. ***The Journal of Immunology*****, 2024, 213: 663–668.**

Opioid use disorder (OUD) and overdose are public health threats, with around 2.7 million individuals aged ≥12 years in the United States suffering from OUD in 2021 and >75% of drug overdose deaths in 2021 involving opioids (1). The COVID-19 pandemic has contributed to an increase in fatal overdoses from synthetic opioids, with 18-fold more fatal overdoses in 2020 than in 2013 (2) and with fatal overdoses totaling 100,000 in 2021 (3). Alarmingly, fentanyl and fentanyl analogues (F/FAs) are often found as adulterants in the illicit drug supply, such as in oxycodone and hydrocodone counterfeit prescription pills, or in cocaine and methamphetamine (4). Current medications for OUD include μ opioid receptor (MOR) agonists such as methadone and buprenorphine and antagonists such as naltrexone. However, these medications require frequent dosing and have side effects that can limit patient compliance (5, 6); hence the risk of relapse for individuals with OUD remains high (7, 8). Similarly, the only Food and Drug Administration (FDA)-approved treatments to reverse opioid overdose, naloxone and nalmefene, have not been sufficient to stop the rise in opioid overdoses, partly because of their reduced effectiveness against highly potent synthetic opioids such as F/FAs and their relatively short half-lives (9, 10). Nalmefene, which was recently approved for overdose reversal by the FDA, has a longer half-life than naloxone (11 h compared with 1.5 h) (11), but it is not yet clear whether this will sufficiently improve patient outcomes. Thus, patients experiencing overdose from F/FAs and other synthetic opioids may require multiple doses of reversal agents (12–14). In addition, opioid antagonists may precipitate withdrawal symptoms, leading to hesitancy from patients to use them (12, 14, 15).

Vaccines and mAbs offer a promising approach to treating opioid overdoses and for potential use in management of OUD (16). Several anti-fentanyl mAbs have been previously shown to prevent fentanyl toxicity in mice (17, 18), and a lead fentanyl-specific mAb, clone HY6-F9, has been further shown to both prevent and reverse fentanyl toxicity in rats (19–21). Another candidate mAb for F/FA has shown efficacy in nonhuman primates (22). Opioid-specific Abs work by binding to the target opioid in the bloodstream and preventing it from crossing the blood-brain barrier (19–21). As compared to MOR-targeting medications, mAbs display a longer serum half-life, and because they do not interfere with endogenous opioid signaling, they are expected to have fewer cognitive side effects. A high and sustained Ab concentration must be present in the bloodstream to ensure sufficient binding to target molecules; hence a significant limitation to mAb-based therapies is the high doses of Abs needed to effectively sequester opioid molecules (6,7). Increasing the serum half-life of IgG mAbs would increase the duration of efficacy, leading to a more cost-effective approach and reducing the burden of compliance on patients by reducing the frequency of dosing.

*Department of Pharmacology, University of Minnesota, Minneapolis, MN; [†]Department of Psychiatry and Behavioral Sciences, University of Washington, Seattle, WA; and [‡]University of Washington Center for Medication Development for Substance Use Disorders, Garvey Institute for Brain Solutions, Seattle, WA

ORCIDs: 0000-0002-2588-0900 (A.K.); 0000-0002-3395-6776 (C.A.B.); 0000-0002-6934-4050 (D.H.); 0000-0003-1036-0184 (M.P.).

Received for publication March 27, 2024. Accepted for publication June 19, 2024.

This work was supported by the National Institute on Drug Abuse Grants U01 DA051658 and UG3DA057850 (to M.P.), Rick L. Seaver Endowed Professorship in Brain Wellness (to M.P.), and Garvey Institute for Brain Health Solutions (to M.P.).

C.A.B. and M.P. participated in research design. A.K. and D.H. conducted experiments. C.A.B., M.D.R., and A.K. conducted data analysis. A.K., C.A.B., M.D.R., and M.P. wrote or edited the manuscript.

Address correspondence and reprint requests to Marco Pravetoni and Carly A. Baehr, Harborview Medical Center, 300 9th Street, Seattle, WA 98104-2499 (M.P.) and University of Minnesota, 312 Church Street SE, Minneapolis, MN 55455-0215 (C.A.B.). E-mail addresses: mprave@uw.edu (M.P.) and cbaehr@umn.edu (C.A.B.)

The online version of this article contains supplemental material.

Abbreviations used in this article: AUC, area under the curve; BLI, biolayer interferometry; C_{max}, maximum concentration; FcRn, neonatal Fc receptor; FDA, Food and Drug Administration; F/FA, fentanyl and fentanyl analogue; hFcRn, human neonatal Fc receptor; MOR, mu opioid receptor; %MPE, percent maximum possible effect; NCA, noncompartmental analysis; OUD, opioid use disorder; Tg, transgenic; Tm, melting temperature; WT, wild-type.

https://doi.org/10.4049/jimmunol.2400170

The neonatal Fc receptor (FcRn) is expressed on hematopoietic and endothelial cells, and is responsible for maintaining serum IgG levels through recycling (23). Following endocytosis of IgG, pH-dependent interaction of the Fc domain of IgG, specifically the C_H2-C_H3 domains, with FcRn traffics IgG into recycling endosomes for release at the cell surface, rescuing IgG molecules from lysosomal degradation (24, 25). Previous studies have shown that Fcγ receptor I–IV functions are not essential for anti-opioid mAb efficacy in rodent models, but that deletion of FcRn in mice reduced the efficacy of both vaccines and mAb by reducing serum persistence of mAb or vaccine-elicited Ab (26). In this study, we selected three sets of mutations in the Fc of human IgG_1 that have been shown to increase serum persistence through increasing binding to FcRn at endosomal pH, promoting recycling of circulating IgG. The Fc mutant L309D/Q311H/N434S (DHS), incorporated on the mAb trastuzumab, showed improved pharmacokinetics compared with wild-type (WT) IgG in transgenic (Tg) mice expressing the human FcRn while maintaining intact effector functions (27). Another well-established Fc mutant, M252Y/S254T/T256E (YTE), has been used in numerous studies as a standard example of an FcRn affinity-enhanced Fc mutant (27–30). The YTE mutant, which reduces dissociation of Fc-FcRn interaction at endosomal pH in motavizumab for treatment of respiratory syncytial virus, showed serum persistence in humans >4-fold higher than WT IgG (30, 31). Finally, the Fc mutant T307Q/Q311V/A378V (DF215) in motavizumab displayed a 30-fold greater affinity for FcRn at pH 6.0 than WT (30).

This study examined the relationship between mAb concentration and efficacy as a model for mAb efficacy over time, and compared the ability of these previously published Fc mutations to increase serum persistence of a lead anti-fentanyl mAb. First, a dose-response study of the lead chimeric fentanyl-specific mAb (HY6-$F9^{WT}$) revealed a significant correlation between mAb concentration and serum sequestration of fentanyl. To assess whether these Fc mutations would enhance the serum persistence of this mAb, we incorporated Fc region mutations in three mutant mAbs: HY6-$F9^{DF215}$, HY6-$F9^{DHS}$, and HY6-$F9^{YTE}$. Half-life–extended anti-fentanyl mAbs exhibited >10-fold greater binding affinity for human FcRn in vitro, while binding to fentanyl was not affected. The mutant mAbs demonstrated equivalent efficacy to the WT mAb during acute fentanyl challenge in mice. Among the tested mAbs, HY6-$F9^{DF215}$ displayed the longest serum persistence in mice expressing human FcRn. Collectively, these results support incorporation of half-life–extending mutations for mAb-based therapeutics under preclinical investigation for OUD.

Materials and Methods

Generation of chimeric half-life–extended H chain expression vectors

DHS (L309D/Q311H/N434S) (27), DF215 (T307Q/Q311V/A378V) (30), and YTE (M252Y/S254T/T256E) (28) mutations were introduced into pcDNA3.4 expression vectors with human IgG_1 constant regions, as described previously (20), using QuikChange Multi Site-Directed Mutagenesis Kit (catalog no. 200514; Agilent Technologies) and confirmed by Sanger sequencing. An anti-fentanyl Ab H chain V region (clone HY6-F9) (19) was cloned into the vectors containing DHS, DF215, and YTE mutations in human IgG_1. In brief, murine variable H chain region sequences were PCR amplified from anti-fentanyl H chain expression vectors with primers containing 15 bp of homologous overlap to the DHS, DF215, and YTE H chain vectors. Gibson assembly was performed to incorporate the PCR-amplified insert into vectors linearized with XhoI and AfeI (New England Biolabs). The partner anti-fentanyl L chain expression vector was previously described and used without modification (20).

Expression and purification of chimeric half-life–extended mAbs

Expression and purification of the HY6-$F9^{DHS}$, HY6-$F9^{DF215}$, and HY6-$F9^{YTE}$ half-life–extended chimeric anti-fentanyl mAbs were performed as described previously (20). In brief, mAbs were expressed using the Expi293 Expression System (catalog no. A14635; Thermo Fisher Scientific). The supernatant was harvested after 7 d, IgG titer was determined by biolayer interferometry (BLI) on an Octet Red 96e (Sartorius) using protein G biosensors, and mAb was purified via Protein A chromatography with an ÄKTA pure (Cytiva) and a HiTrap MabSelect PrismA column (product no. 17549851; Cytiva). SDS-PAGE was used for confirmatory analysis of the purified mAbs under reducing and nonreducing conditions.

Kinetic analysis of fentanyl-specific mAbs against human FcRn and fentanyl

WT and mutant mAbs were assessed for binding affinity to His-tagged human FcRn (hFcRn; catalog no. FCN-H52W7; Acro Biosystems) and fentanyl hapten using BLI on an Octet Red96e (Sartorius). Biotinylated anti–penta-His mAb (catalog no. 1019225; Qiagen) was immobilized on streptavidin-coated biosensors (catalog no. 18–1509; Sartorius). Buffer used for all sample dilution and baseline steps was 1X PBS (catalog no. P32060; Research Products International), pH 5.8, with 1X kinetics buffer (catalog no. 18–1105; Sartorius). A total of 5 μg/ml biotinylated anti-His mAb was loaded onto biosensors, followed by loading of 50 nM His-tagged hFcRn. Then mutant or WT anti-fentanyl mAbs were loaded at 20, 100, and 200 nM, and their association with hFcRn was measured for 60 s at endosomal pH, followed by their dissociation for 300 s. To confirm that mutations did not affect fentanyl affinity of the mAbs, we measured binding of anti-fentanyl mAb to a biotinylated fentanyl-based hapten as described previously (20). All calculations were performed using the Octet analysis software (Data Acquisition v12.0.0.11; ForteBio), and affinity (K_D) was calculated as the ratio of the dissociation and association rates.

Animals

All experiments were approved by the Institutional Animal Care and Use Committee of the University of Minnesota and were conducted according to the *Guide for the Care and Use of Laboratory Animals*, 8th ed. Male BALB/c mice (Envigo) and male Tg276 mice (FcRn knockout/hFcRn Tg; stock no. 004919; Jackson Laboratory) were 6–9 wk old upon arrival. B6.Cg-$Fcgr^{ttm1Dcr}$ Tg(CAG-FCGRT)276Dcr/DcrJ mice, hemizygous for human *FCGRT*, are commonly used to differentiate small differences in serum half-life (31). Mice were housed in groups of four under standard conditions with a 14/10 h light/dark cycle and provided food and water ad libitum. The animals were acclimated to the housing conditions for 1 wk before the start of the experiments.

In vivo efficacy of mAbs against fentanyl-induced toxicity

Mice (BALB/c, $n = 4$/group) were randomized to receive 2–40 mg/kg WT mAb via i.p. injection in one experiment, or 40 mg/kg WT or mutant mAb in other experiments, as noted in each figure. For determination of mAb efficacy, 24 h after immunization, the mice were challenged with 0.1 mg/kg fentanyl s.c. Thirty minutes after fentanyl exposure, mice were assessed for fentanyl-induced bradycardia and respiratory depression using a MouseOx Plus pulse oximeter (Starr Life Science) and for antinociception by latency to respond on a hot plate set at 54°C (Columbus Instruments) to a maximum of 60 s. Behavioral assessments were performed by experimenters who were blinded to treatment conditions. After behavioral assessments, the animals were euthanized by CO_2 inhalation. The serum and brain were then collected from the mice to measure fentanyl distribution in the brain by liquid chromatography-mass spectrometry as described previously (19, 32, 33).

Quantitation of Ab titers by ELISA

For determination of Ab levels in mAb efficacy experiments, blood was sampled 1 h prior to fentanyl challenge. For assessment of mAb half-life, Tg276 mice were passively immunized with 40 mg/kg WT or mutant mAb i.p., and blood was sampled at 1, 7, 14, 28, and 35 d postimmunization by submandibular bleeding. Serum Ab titers were evaluated by ELISA (19, 32). High-binding 96-well plates were coated with a fentanyl-based hapten conjugated to BSA (0.05 μg/ml), along with a negative control coating of unconjugated BSA in carbonate buffer (catalog no. C3041; Sigma). The plates were then washed with PBS-T and blocked with 1% porcine gelatin (catalog no. G2500; Sigma). The plates were then incubated with serially diluted serum samples from experimental mice, or purified mAb as a reference standard, for 2 h. Plates were washed with PBS-T, and then HRP-conjugated anti-human IgG secondary Ab (catalog no. 10320; Alpha Diagnostic International) was applied to the plate to detect fentanyl-specific serum IgG levels.

The plates were read using a SigmaFast OPD substrate (catalog no. P9187; Sigma) on a microplate reader (Infinite M1000; Tecan).

Statistical analysis

Statistical analyses were performed using Prism v9.2 (GraphPad, San Diego, CA). Percent maximum possible effect (%MPE) versus serum concentration was analyzed for correlation using simple linear regression. %MPE, bradycardia, respiratory depression, and brain and serum fentanyl were compared between groups using one-way ANOVA followed by Dunnett's multiple comparisons test.

Estimation of pharmacokinetic parameters of mAbs

Pharmacokinetic parameters of mAbs were estimated with PKSolver 2.0 (34) using noncompartmental analysis (NCA). PKSolver has been demonstrated to perform equally to Phoenix WinNonlin (Certara, Radnor, PA) (35), the gold standard for pharmacokinetic analysis. NCA was chosen because it requires the fewest assumptions compared with model-based approaches (36). Curve fits were visualized in Fig. 4 using $\log(y) = mx + \log(k)$, where y is the mAb concentration, m is the slope, x is time, and k is the y-intercept.

Results

Characterization of fentanyl-specific mAbs

HY6-F9^{WT}, HY6-F9^{DHS}, HY6-F9^{DF215}, and HY6-F9^{YTE} mAbs (Fig. 1) were recombinantly expressed, purified, and assessed for properties including thermal stability and binding to fentanyl. The mAb melting temperature (T_m) was tested as a measure of thermal stability (Supplemental Fig. 1). All mAbs showed similar T_m in the Fab domain (HY6-F9^{WT}: 76.8°C; HY6-F9^{DF215}: 75.9°C; HY6-F9^{DHS}: 76.1°C; HY6-F9^{YTE}: 76.5°C), whereas HY6-F9^{DHS} showed increased T_m and HY6-F9^{YTE} showed decreased T_m in the CH2 domain (HY6-F9^{WT}: 66.4°C; HY6-F9^{DF215}: 65.9°C; HY6-F9^{DHS}: 70.1°C; HY6-F9^{YTE}: 57.5°C). The binding affinity of the WT and half-life–extended mAbs for fentanyl hapten F_1 showed no detectable differences, with all mAbs showing $K_D <$ 0.01 nM by BLI, consistent with the previously reported K_D of HY6-F9 (20). HY6-F9^{WT} showed no aggregation, and mutant mAbs showed 4–7% aggregation by size exclusion chromatography (Supplemental Fig. 2).

Mutations increase binding of fentanyl-specific mAbs to hFcRn in vitro

To investigate the potential effects of the WT and half-life–extended mAbs on their interaction with hFcRn in the endosomal environment, we employed BLI to determine the affinity of each mAb to the hFcRn at pH 5.8. The three mutant anti-fentanyl mAbs exhibited increased binding affinity for hFcRn compared with the WT mAb (Table I). HY6-F9^{DF215} demonstrated the highest binding affinity for the hFcRn at 1.97 nM, followed by HY6-F9^{DHS} and HY6-F9^{YTE} at 3.63 and 2.72 nM, respectively. In contrast, HY6-F9^{WT} displayed the lowest binding affinity to hFcRn, at 163 nM.

Anti-fentanyl mAb reduces fentanyl effects in a dose-dependent manner

To determine the minimally effective dose of the lead WT fentanyl-specific mAb, we passively immunized mice i.p. with 2–40 mg/kg WT mAb and challenged with a 0.1 mg/kg dose of fentanyl. Serum mAb concentrations correlated with reduced fentanyl-induced antinociception (Fig. 2A), and anti-fentanyl mAb reduced the distribution of fentanyl to the brain and increased the serum fentanyl concentrations in a dose-dependent manner (Fig. 2B, 2C). At all mAb doses, there was a significant reduction of brain fentanyl levels by 40 to >95%. At higher mAb doses (30 and 40 mg/kg), only very low levels of fentanyl in brain were detected.

Half-life–extended fentanyl-specific mAbs show equivalent efficacy to WT

To evaluate whether anti-fentanyl mAbs were effective in reducing fentanyl distribution to the brain in vivo, we passively immunized mice i.p. with saline (control) or 40 mg/kg HY6-F9^{WT}, HY6-F9^{DHS}, HY6-F9^{DF215}, and HY6-F9^{YTE} mAb and challenged with 0.1 mg/kg fentanyl. Passive immunization with anti-fentanyl mAbs significantly reduced fentanyl-induced antinociception ($p < 0.0001$), bradycardia ($p < 0.05$), and respiratory depression ($p < 0.05$) compared with saline (Fig. 3A–C). No significant differences among mAb-treated groups were apparent (antinociception: $p > 0.67$, bradycardia: $p > 0.72$, breath rate: $p > 0.71$ for all groups compared with WT). Serum level of mAb was tested by ELISA prior to challenge, and HY6-F9^{WT}–treated mice showed significantly higher serum mAb concentrations than HY6-F9^{DF215} ($p = 0.0142$) and HY6-F9^{YTE} ($p = 0.0165$) groups (Fig. 3D). The serum mAb concentration of HY6-F9^{DHS} was not significantly different from HY6-F9^{WT} ($p = 0.2055$). Fentanyl distribution to the brain was significantly reduced in all mAb groups compared with that in the saline control group (Fig. 3E), with no significant differences among mAb-treated groups ($p > 0.55$).

Mutant fentanyl-specific mAbs show increased half-life in vivo

Tg276 mice expressing hFcRn were passively immunized i.p. with a 40 mg/kg dose of HY6-F9^{WT}, HY6-F9^{DHS}, HY6-F9^{DF215}, or HY6-F9^{YTE} mAb, and blood samples were collected over time to measure fentanyl-specific serum IgG (Fig. 4). All mutant mAbs exhibited higher serum levels and higher maximum concentration (C_{max}) and area under the curve (AUC) (Table I) compared with HY6-F9^{WT}. The half-life of HY6-F9^{YTE} mAb was not significantly longer than that of HY6-F9^{WT}, whereas HY6-F9^{DHS} exhibited a 2-fold increase relative to HY6-F9^{WT}. HY6-F9^{DF215} demonstrated the

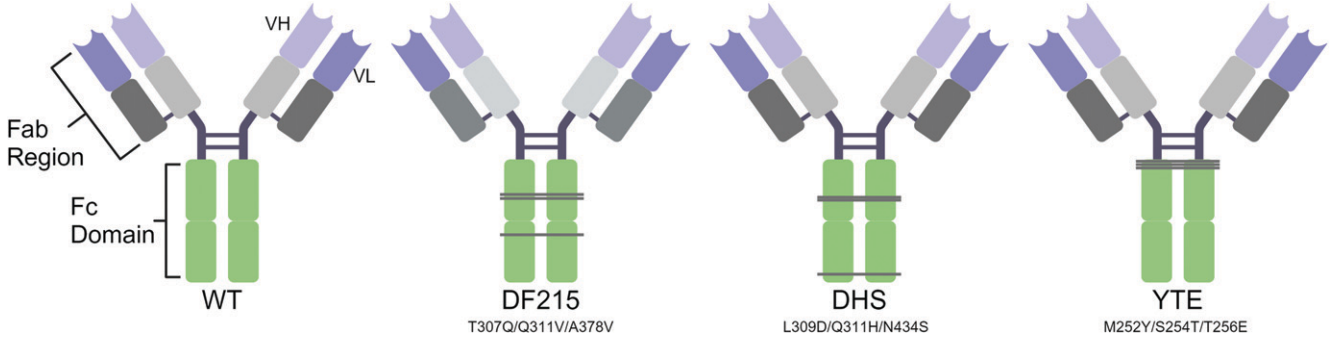

FIGURE 1. Illustration of chimeric fentanyl-specific mAbs with locations of Fc mutations. The purple chain of the Fab region represents the murine H and L chain, whereas the gray chain indicates the human H and L chain. The human Fc domain is green, and the general locations of the mutations introduced are denoted by dark gray lines.

Table I. Binding affinity and pharmacokinetic profile of fentanyl-specific chimeric mAbs

mAb	hFcRn K_D (nM)	Half-life (d)	C_{max} (μg/ml)	AUC (h·μg/ml)	Volume of Distribution (l/kg)	Clearance (ml/min·kg)
HY6-F9^{WT}	163 ± 20	6.3	76.7	13.7	620.9	47.6
HY6-F9^{DF215}	1.97 ± 0.04	26.4	257.7	69.3	352.7	6.4
HY6-F9^{DHS}	3.63 ± 0.10	14.7	108.3	41.5	397.7	13.1
HY6-F9^{YTE}	2.72 ± 0.06	6.9	173.7	46.5	203.0	14.1

Binding affinity of fentanyl-specific chimeric mAbs for hFcRn was performed by BLI. Pharmacokinetic parameters were estimated using NCA with PKSolver 2.0.

highest serum persistence, with a 4-fold increase in half-life compared with HY6-F9^{WT} and a serum concentration of 37.5 μg/ml 35 d after administration.

Discussion

The goal of this work was to establish proof of concept for use of mutations in the Fc region for extending the duration of therapeutic efficacy of anti-fentanyl mAbs. Previous studies with opioid mAbs implicated FcRn as critical for efficacy in mice (26). This study used three sets of mutations, which were previously shown to increase FcRn binding and extend the half-life of therapeutic mAbs, and directly compared their effect on efficacy and pharmacokinetics of a lead chimeric fentanyl-specific mAb. The key findings of this study were (1) mutations on the Fc portion of anti-fentanyl mAbs increased their binding to hFcRn in vitro, (2) anti-fentanyl blockade by mAb was preserved in Fc mutant mAbs, and (3) the DF215 mutant showed the highest affinity for hFcRn and the longest half-life in vivo. These data highlight the benefits of extending mAb half-life while preserving its efficacy in vivo. The DF215, DHS, and YTE mutations were previously studied with trastuzumab, motavizumab, and others (27–30) with similar effects, and they demonstrate the generalizability of these mutations to improve characteristics of other mAbs, including anti-fentanyl and other opioid-targeting mAbs. Several Fc-engineered therapeutic Abs have been evaluated in clinical trials (37), and the YTE-containing nirsevimab was approved by the FDA in 2023, supporting the exploration of FcRn-targeting mutations for anti-opioid mAbs under preclinical investigation (38).

An in vivo dose-response study was first performed to model the decrease in mAb concentration across multiple half-lives. Surprisingly, doses down to 2 mg/kg HY6-F9^{WT} reduced fentanyl-induced antinociception, whereas 5 mg/kg mAb was the minimum dose that significantly increased fentanyl levels in serum. This expands upon several previous studies that demonstrated correlations between individual variations in vaccine-elicited Abs and efficacy of fentanyl vaccines (39, 40), and studies of fentanyl-specific mAbs that tested dose dependence of mAb efficacy in a more limited capacity (17, 41). Collectively, these studies serve to highlight the stoichiometric sequestration mechanism of mAb against fentanyl. Notably, as a ratio relative to the fentanyl dose of 0.1 mg/kg, the mAb doses tested in this study range from a 2-fold molar excess of mAb (40 mg/kg mAb) to an 11-fold molar excess of fentanyl (2 mg/kg mAb). Hence these results highlight that even small doses of this mAb are sufficient to reduce brain concentrations of fentanyl and to blunt the effects of the drug. Such data could inform single ascending dose studies in clinical trials of mAb against fentanyl and other opioids of interest.

All mutant mAbs were as effective as HY6-F9^{WT} in blocking fentanyl-induced effects. However, these mutant mAbs appeared to show a slight, nonsignificant trend toward reduced efficacy compared with the WT mAb, which may have been because of lower Ab levels during fentanyl challenge. The lower serum concentration of the mutant mAbs is possibly due to the use of BALB/c mice. Although murine FcRn shares homology with hFcRn and is able to bind human IgG_1 (42), it is not clear to what extent the mutations used in this study affect binding to murine FcRn. Despite these differences in mAb levels, the mutant mAbs successfully blunted fentanyl effects and demonstrated that these mutations preserved the protective effects of an anti-fentanyl mAb while improving Ab characteristics.

HY6-F9^{DF215} showed the highest affinity for hFcRn of the mutants tested, and exhibited the longest half-life, highest C_{max}, and highest AUC in hFcRn-expressing mice. Although HY6-F9^{YTE} showed high hFcRn affinity, and the C_{max} and AUC of this mutant were higher than HY6-F9^{WT}, its in vivo half-life was similar to HY6-F9^{WT}. The reduced half-life of HY6-F9^{YTE} could be because of its low thermal stability (Supplemental Fig. 2), which was consistent with previously published studies of YTE mutants (28). The half-life of WT IgG Abs in humans is ∼10–21 d in circulation, depending on the subtype (30,43), and because a 5 mg/kg mAb dose (similar to the expected levels of mAb three half-lives after a 40 mg/kg dose) blunted the effects of fentanyl, a dose of 40 mg/kg mAb would theoretically be effective against fentanyl for 2 mo, or much longer for Fc mutants. In comparison, the MOR partial agonist buprenorphine has an estimated half-life of 24–60 h, whereas

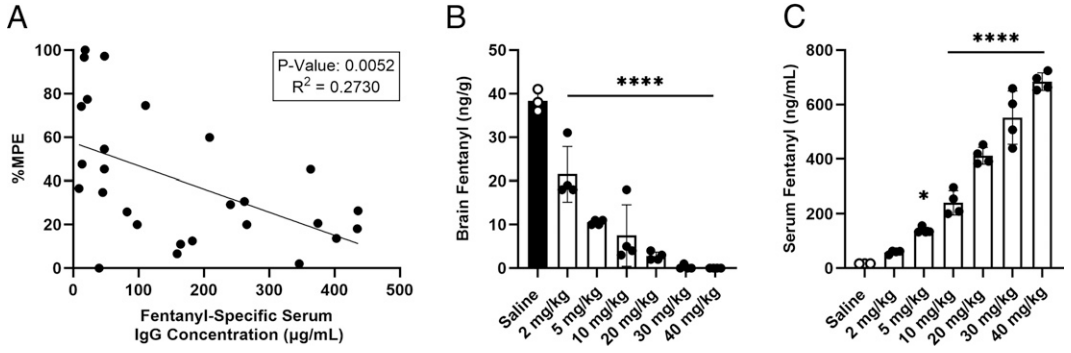

FIGURE 2. Dose-dependent efficacy of anti-fentanyl mAb. BALB/c mice (n = 4 male mice per group) were passively immunized i.p. with 2–40 mg/kg HY6-F9^{WT}. After 24 h, blood was collected to quantify serum IgG concentration, and mice were challenged with 0.1 mg/kg fentanyl s.c. and evaluated for fentanyl-induced antinociception on a hot plate as %MPE (**A**). Brain (**B**) and blood (**C**) were collected to measure fentanyl distribution. Data are mean ± SD. Asterisks indicate significance: *$p < 0.05$, ****$p < 0.0001$, compared with saline control.

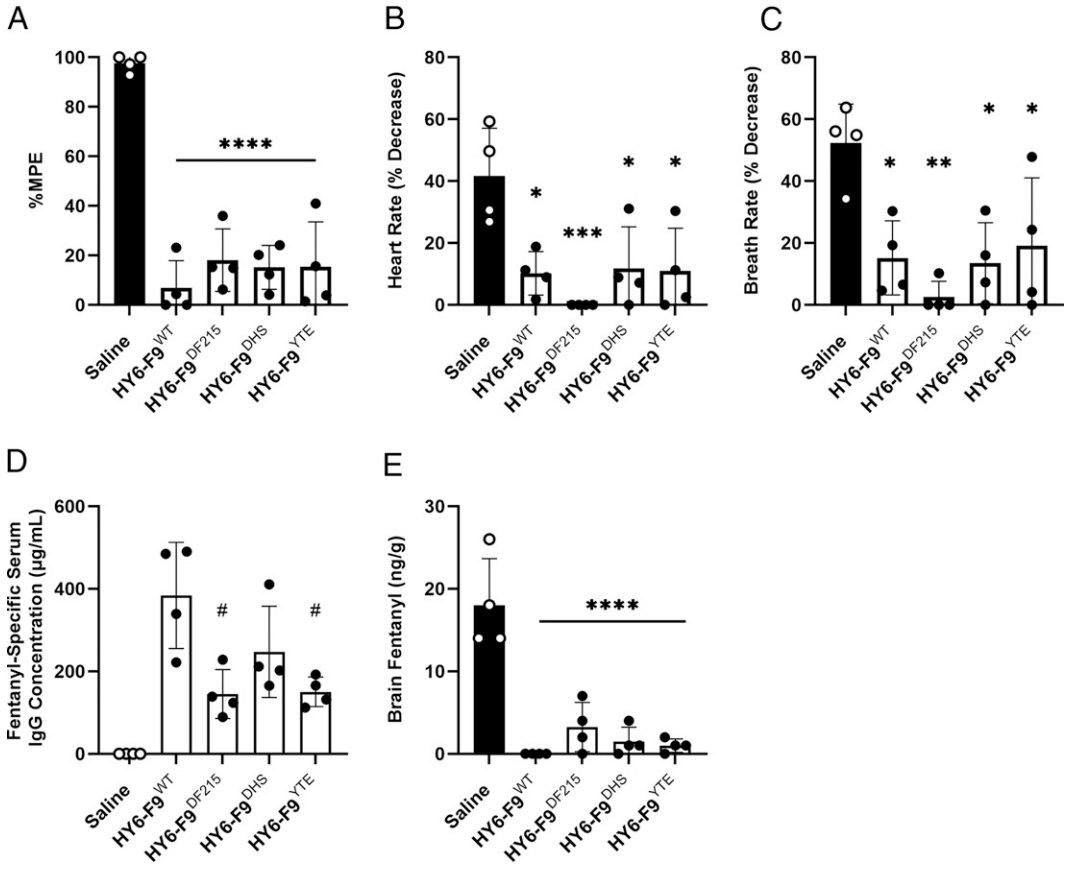

FIGURE 3. In vivo efficacy of WT and mutant mAbs against fentanyl-induced toxicity. BALB/c mice ($n = 4$ male mice per group) were passively immunized i.p. with 40 mg/kg WT or mutant mAb displaying life-extending mutations. At 24 h posttreatment, mice were challenged with 0.1 mg/kg fentanyl s.c. Thirty minutes after fentanyl exposure, mice were assessed for antinociception as %MPE (**A**), bradycardia (**B**), and respiratory depression (**C**). Serum was collected prior to fentanyl exposure to measure Ab concentration (**D**). Brain was collected to measure fentanyl distribution (**E**). Data are mean ± SD. Symbols indicate significance: $*p < 0.05$, $**p < 0.01$, $***p < 0.001$, $****p < 0.0001$, compared with saline control; $^{\#}p < 0.05$, compared with WT.

naltrexone has an estimated half-life of 5–10 d when given i.m., although extended-release formulations of naltrexone are available as a monthly injectable used for OUD. Therefore, half-life–extended mAbs could compare favorably with available OUD medications.

There are several limitations to this study, including that the HY6-F9 used in this study is chimeric and not fully humanized. Because chimeric mAbs are not ideal for use in humans in vivo due to potential immunogenicity, future work will include testing DF215 or other mutations with the humanized lead mAb HY6-F9_Hu, which previously showed equivalent efficacy to chimeric HY6-F9 in rats (20). Also, the Tg mouse model used for determination of mAb half-life, Tg276, expresses the human *FCGRT* gene under a constitutive promoter (44); these mice overexpress hFcRn, which allows the detection of minor variations in Ab persistence in vivo. Although this model may be less directly predictive of pharmacokinetics of therapeutic mAbs in humans compared with the equivalent strain with *FCGRT* under its native promoter (Tg32), the half-life of mAbs in Tg276 mice tends to be lower than in humans; hence it can be expected that the mutant HY6-F9 mAbs will have favorable serum persistence. Finally, with the exception of the study shown in Fig. 2, fixed doses of mAb and fentanyl were used to assess in vivo efficacy. Meanwhile, in a clinical scenario of OUD or overdose, the dose and identity of opioid may be unknown. However, the fentanyl dose used in this study, 0.1 mg/kg, is 10–50× higher than doses used to produce analgesia in humans. Hence, moderate to high doses of mAb may be sufficient to protect against probable fentanyl exposure scenarios for an extended period.

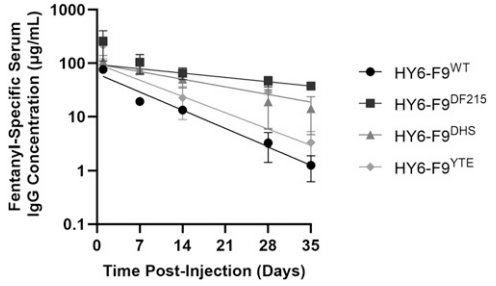

FIGURE 4. In vivo evaluation of serum half-life of WT and mutant mAbs. Tg276 Tg mice ($n = 4$ male mice per group) expressing the humanized FcRn were passively immunized i.p. with 40 mg/kg WT or mutant mAb. Blood was collected on days 1, 7, 14, 28, and 35 to measure serum IgG concentrations. NCA was performed to estimate pharmacokinetic parameters, and curve fits were generated using $\log(y) = mx + \log(k)$. Data are mean ± SD.

In conclusion, with the unprecedented surge in opioid-related overdose fatalities, it has become increasingly evident that both improved access to existing medications and development of new therapeutic interventions are imperative to address this epidemic. The development of effective and long-lasting biologics for OUD would have a significant impact on the lives of those grappling with opioid addiction and who are at risk for relapse. This study identified a promising anti-fentanyl mAb candidate with Fc mutations, HY6-F9^{DF215}, which protected against fentanyl effects and showed a 4-fold increased half-life in mice. This approach could generalize

to mAbs targeting other opioids or drugs of abuse that have candidate mAbs in preclinical to clinical development.

Acknowledgments

We thank Diego Luengas and Jennifer Vigliaturo for invaluable assistance. Some figures were created using BioRender.com.

Disclosures

The mAbs described in this work are the subject of patent applications (inventors: M.P., C.A.B., and D.H.). M.P. is the founder of CounterX Therapeutics, Inc. The other authors have no financial conflicts of interest.

References

1. Center for Behavioral Health Statistics and Quality. 2021. Results from the 2020 national survey on drug use and health: detailed tables. Rockville, MD: Substance Abuse and Mental Health Services Administration. Available at: https://www.samhsa.gov/data/.
2. CDC. 2022. Death rates for drug overdose among persons aged 25–44 Years, by race and ethnicity— United States, 2000–2020. *MMWR Morb. Mortal. Wkly. Rep.* 71: 1485.
3. Spencer, M. R., A. M. Miniño, and M. Warner. 2022. Drug overdose deaths in the United States, 2001–2021. NCHS Data Brief, no. 457. Hyattsville, MD: National Center for Health Statistics. Available at: https://dx.doi.org/10.15620/cdc:122556.
4. Fischer, B., C. Russell, Y. Murphy, and P. Kurdyak. 2015. Prescription opioids, abuse and public health in Canada: Is fentanyl the new centre of the opioid crisis? *Pharmacoepidemiol. Drug Saf.* 24: 1334–1336.
5. Stöver, H. J. 2012. Outcomes of opioid-dependence treatment across Europe: Identifying opportunities for improvement. *Heroin Addict. Relat. Clin. Probl.* 14: 39–50.
6. Gilman, M., L. Li, K. Hudson, T. Lumley, G. Myers, C. Corte, and R. Littlewood. 2018. Current and future options for opioid use disorder: A survey assessing real-world opinion of service users on novel therapies including depot formulations of buprenorphine. *Patient Prefer. Adherence* 12: 2123–2129.
7. Veilleux, J. C., P. J. Colvin, J. Anderson, C. York, and A. J. Heinz. 2010. A review of opioid dependence treatment: Pharmacological and psychosocial interventions to treat opioid addiction. *Clin. Psychol. Rev.* 30: 155–166.
8. Chang, Y. P., and T. Raynor. 2021. Factors associated with relapse in individuals with opioid use disorder receiving suboxone in rural areas. *J. Addict. Nurs.* 32: 20–26.
9. Seidler, D., G. H. Stühlinger, G. Fischer, C. Woisetschlaeger, A. Berzlanovich, R. Schmid, M. M. Hirschl, and A. N. Laggner. 1996. After antagonization of acute opiate overdose: A survey at hospitals in Vienna. *Addiction* 91: 1479–1487.
10. Caudarella, A., H. Dong, M. J. Milloy, T. Kerr, E. Wood, and K. Hayashi. 2016. Non-fatal overdose as a risk factor for subsequent fatal overdose among people who inject drugs. *Drug Alcohol Depend.* 162: 51–55.
11. Wang, D. S., G. Sternbach, and J. Varon. 1998. Nalmefene: A long-acting opioid antagonist. *J. Emerg. Med.* 16: 471–475.
12. Abdelal, R., A. Raja Banerjee, S. Carlberg-Racich, N. Darwaza, D. Ito, J. Shoaff, and J. Epstein. 2022. Real-world study of multiple naloxone administration for opioid overdose reversal among bystanders. *Harm. Reduct. J.* 19: 49.
13. Faul, M., P. Lurie, J. M. Kinsman, M. W. Dailey, C. Crabaugh, and S. M. Sasser. 2017. Multiple naloxone administrations among emergency medical service providers is increasing. *Prehosp. Emerg. Care* 21: 411–419.
14. Moss, R. B., and D. J. Carlo. 2019. Higher doses of naloxone are needed in the synthetic opiod era. *Subst. Abuse Treat. Prev. Policy* 14: 6.
15. Shaw, L. V., J. Moe, R. Purssell, J. A. Buxton, J. Godwin, M. M. Doyle-Waters, P. M. A. Brasher, J. P. Hau, J. Curran, C. M. Hohl, et al. 2019. Naloxone interventions in opioid overdoses: A systematic review protocol. *Syst. Rev.* 8: 138.
16. Pravetoni, M., and S. D. Comer. 2019. Development of vaccines to treat opioid use disorders and reduce incidence of overdose. *Neuropharmacology* 158: 107662.
17. Smith, L. C., P. T. Bremer, C. S. Hwang, B. Zhou, B. Ellis, M. S. Hixon, and K. D. Janda. 2019. Monoclonal antibodies for combating synthetic opioid intoxication. *J. Am. Chem. Soc.* 141: 10489–10503.
18. Ban, B., R. C. Barrientos, T. Oertel, E. Komla, C. Whalen, M. Sopko, Y. You, P. Banerjee, A. Sulima, A. E. Jacobson, et al. 2021. Novel chimeric monoclonal antibodies that block fentanyl effects and alter fentanyl biodistribution in mice. *MAbs.* 13: 1991552.
19. Baehr, C., A. H. Kelcher, A. Khaimraj, D. E. Reed, S. G. Pandit, D. AuCoin, S. Averick, and M. Pravetoni. 2020. Monoclonal antibodies counteract opioid-induced behavioral and toxic effects in mice and rats. *J. Pharmacol. Exp. Ther.* 375: 469–477.
20. Hicks, D., C. Baehr, P. Silva-Ortiz, A. Khaimraj, D. Luengas, F. A. Hamid, and M. Pravetoni. 2022. Advancing humanized monoclonal antibody for counteracting fentanyl toxicity towards clinical development. *Hum. Vaccin. Immunother.* 18: 2122507.
21. Baehr, C. A., M. M. Wu, S. G. Pandit, J. Arias-Umana, D. AuCoin, and M. Pravetoni. 2022. Pharmacological profiling of antifentanyl monoclonal antibodies in combination with naloxone in pre- and postexposure models of fentanyl toxicity. *J. Pharmacol. Exp. Ther.* 381: 129–136.
22. Bremer, P. T., E. L. Burke, A. C. Barrett, and R. I. Desai. 2023. Investigation of monoclonal antibody CSX-1004 for fentanyl overdose. *Nat. Commun.* 14: 7700.
23. Pyzik, M., T. Rath, W. I. Lencer, K. Baker, and R. S. Blumberg. 2015. FcRn: The architect behind the immune and nonimmune functions of IgG and albumin. *J. Immunol.* 194: 4595–4603.
24. Ghetie, V., and E. S. Ward. 2000. Multiple roles for the major histocompatibility complex class I-related receptor FcRn. *Annu. Rev. Immunol.* 18: 739–766.
25. Ramdani, Y., J. Lamamy, H. Watier, and V. Gouilleux-Gruart. 2022. Monoclonal antibody engineering and design to modulate FcRn activities: A comprehensive review. *Int. J. Mol. Sci.* 23: 9604.
26. Huseby Kelcher, A. M., C. A. Baehr, F. A. Hamid, G. T. Hart, and M. Pravetoni. 2021. Contribution of antibody-mediated effector functions to the mechanism of efficacy of vaccines for opioid use disorders. *J. Immunol.* 207: 860–867.
27. Lee, C.-H., T. H. Kang, O. Godon, M. Watanabe, G. Delidakis, C. M. Gillis, D. Sterlin, D. Hardy, M. Cogné, L. E. Macdonald, et al. 2019. An engineered human Fc domain that behaves like a pH-toggle switch for ultra-long circulation persistence. *Nat. Commun.* 10: 5031.
28. Dall'Acqua, W. F., P. A. Kiener, and H. Wu. 2006. Properties of human IgG1s engineered for enhanced binding to the neonatal Fc Receptor (FcRn). *J. Biol. Chem.* 281: 23514–23524.
29. Dall'Acqua, W. F., R. M. Woods, E. S. Ward, S. R. Palaszynski, N. K. Patel, Y. A. Brewah, H. Wu, P. A. Kiener, and S. Langermann. 2002. Increasing the affinity of a human IgG1 for the neonatal Fc receptor: biological consequences. *J. Immunol.* 169: 5171–5180.
30. Booth, B. J., B. Ramakrishnan, K. Narayan, A. M. Wollacott, G. J. Babcock, Z. Shriver, and K. Viswanathan. 2018. Extending human IgG half-life using structure-guided design. *MAbs.* 10: 1098–1110.
31. Petkova, S. B., S. Akilesh, T. J. Sproule, G. J. Christianson, H. Al Khabbaz, A. C. Brown, L. G. Presta, Y. G. Meng, and D. C. Roopenian. 2006. Enhanced half-life of genetically engineered human IgG1 antibodies in a humanized FcRn mouse model: Potential application in humorally mediated autoimmune disease. *Int. Immunol.* 18: 1759–1769.
32. Robinson, C., V. Gradinati, F. Hamid, C. Baehr, B. Crouse, S. Averick, M. Kovaliov, D. Harris, S. Runyon, F. Baruffaldi, et al. 2020. Therapeutic and prophylactic vaccines to counteract fentanyl use disorders and toxicity. *J. Med. Chem.* 63: 14647–14667.
33. Raleigh, M. D., M. Pravetoni, A. C. Harris, A. K. Birnbaum, and P. R. Pentel. 2013. Selective effects of a morphine conjugate vaccine on heroin and metabolite distribution and heroin-induced behaviors in rats. *J. Pharmacol. Exp. Ther.* 344: 397–406.
34. Zhang, Y., M. Huo, J. Zhou, and S. Xie. 2010. PKSolver: An add-in program for pharmacokinetic and pharmacodynamic data analysis in Microsoft Excel. *Comput. Methods Programs Biomed.* 99: 306–314.
35. Averick, S. E., A. J. Kassick, D. Song, B. Zhang, J. Vigliaturo, D. Luengas, P. Silva-Ortiz, M. Pravetoni, and M. D. Raleigh. 2024. Evaluating the rate of reversal of fentanyl-induced respiratory depression using a novel long-acting naloxone nanoparticle, cNLX-NP. *Front. Psychiatry* 15: 1366186.
36. Gabrielsson, J., and D. Weiner. 2012. Non-compartmental analysis. *Methods Mol. Biol*. 929: 377–389.
37. Ko, S., M. Jo, and S. T. Jung. 2021. Recent achievements and challenges in prolonging the serum half-lives of therapeutic IgG antibodies through Fc engineering. *BioDrugs* 35: 147–157.
38. Sun, M., H. Lai, F. Na, S. Li, X. Qiu, J. Tian, Z. Zhang, and L. Ge. 2023. Monoclonal antibody for the prevention of respiratory syncytial virus in infants and children: A systematic review and network meta-analysis. *JAMA Netw. Open* 6: E230023.
39. Stone, A. E., S. E. Scheuermann, C. N. Haile, G. D. Cuny, M. L. Velasquez, J. P. Linhuber, A. L. Duddupudi, J. R. Vigliaturo, M. Pravetoni, T. A. Kosten, et al. 2021. Fentanyl conjugate vaccine by injected or mucosal delivery with dmLT or LTA1 adjuvants implicates IgA in protection from drug challenge. *NPJ Vaccines* 6: 69.
40. Crouse, B., C. Robinson, A. Huseby Kelcher, M. Laudenbach, J. E. Abrahante, and M. Pravetoni. 2020. Mechanisms of interleukin 4 mediated increase in efficacy of vaccines against opioid use disorders. *NPJ Vaccines* 5: 99.
41. Triller, G., E. P. Vlachou, H. Hashemi, M. van Straaten, J. P. Zeelen, Y. Kelemen, C. Baehr, C. L. Marker, S. Ruf, A. Svirina, et al. 2023. A trypanosome-derived immunotherapeutics platform elicits potent high-affinity antibodies, negating the effects of the synthetic opioid fentanyl. *Cell Rep.* 42: 112049.
42. Ober, R. J., C. G. Radu, V. Ghetie, and E. S. Ward. 2001. Differences in promiscuity for antibody-FcRn interactions across species: implications for therapeutic antibodies. *Int. Immunol.* 13: 1551–1559.
43. Morell, A., W. D. Terry, and T. A. Waldmann. 1970. Metabolic properties of IgG subclasses in man. *J. Clin. Invest.* 49: 673–680.
44. Avery, L. B., M. Wang, M. S. Kavosi, A. Joyce, J. C. Kurz, Y.-Y. Fan, M. E. Dowty, M. Zhang, Y. Zhang, A. Cheng, et al. 2016. Utility of a human FcRn transgenic mouse model in drug discovery for early assessment and prediction of human pharmacokinetics of monoclonal antibodies. *MAbs* 8: 1064–1078.